Biomaterials 33 (2012) 2007–2015

Contents lists available at SciVerse ScienceDirect

Biomaterials

journal homepage: www.elsevier.com/locate/biomaterials

Dynamics of T cells on endothelial layers aligned by nanostructured surfaces

Kwang Hoon Song [a,1], Keon Woo Kwon [a,d,1], Sukhyun Song [f], Kahp-Yang Suh [d,e,**], Junsang Doh [a,b,c,*]

[a] Department of Mechanical Engineering, Pohang University of Science and Technology (POSTECH), San 31, Hyoja-dong, Nam-Gu, Pohang, Gyeongbuk 790-784, South Korea
[b] School of Interdisciplinary Bioscience and Bioengineering (I-Bio), Pohang University of Science and Technology (POSTECH), San 31, Hyoja-dong, Nam-Gu, Pohang, Gyeongbuk 790-784, South Korea
[c] World Class University Program Division of Integrative Biosciences and Biotechnology (IBB), Pohang University of Science and Technology (POSTECH), San 31, Hyoja-dong, Nam-Gu, Pohang, Gyeongbuk 790-784, South Korea
[d] School of Mechanical and Aerospace Engineering, Seoul National University, Seoul 151-742, South Korea
[e] World Class University Program on Multiscale Mechanical Design, Seoul National University, Seoul 151-742, South Korea
[f] Department of Mechanical Engineering, KAIST, Daejeon, South Korea

ARTICLE INFO

Article history:
Received 19 October 2011
Accepted 2 December 2011
Available online 19 December 2011

Keywords:
Nanostructured surfaces
Capillary force lithography
Endothelial cell alignment
T cell dynamics
Transendothelial migration

ABSTRACT

In this work, well-aligned endothelial cell (EC) layers were prepared by culturing ECs on surfaces containing nanoscale ridges/grooves fabricated by UV-assisted capillary force lithography. Then, the dynamics of T cells on well-aligned ECs were compared with that on randomly oriented ECs cultured on flat surfaces. With this experimental setting, we demonstrated for the first time that EC alignment is important for the regulation of transendothelial migration (TEM) of T cells, a critical step for leukocyte infiltration; T cells preferentially underwent TEM at the junctions surrounded by more than three ECs only if ECs surrounding those junctions were poorly aligned. As a result, TEM of T cells occurred more quickly and frequently on randomly oriented ECs cultured on flat surfaces than on well-aligned ECs cultured on nanostructured surfaces. This result will suggest a new strategy for the design of synthetic small diameter vascular grafts and extend our current knowledge of leukocyte dynamics on an inflamed endothelium.

1. Introduction

Leukocytes, or white blood cells, circulating blood vessels recognize signatures of inflammation in blood vessels and initiate dynamic interactions with inflamed endothelia to eventually move out of the blood vessels and enter into inflamed tissues [1–3]. Tissue-infiltrated leukocytes perform various immune functions to eliminate pathogens, but at the same time they can also destroy our own tissues to cause autoimmune diseases such as type 1 diabetes, rheumatoid arthritis, and asthma [3,4]. In addition, accumulation of endothelia-infiltrated leukocytes in blood vessels can cause atherosclerosis and vascular graft rejection [5,6]. Therefore, understanding the dynamics of leukocytes in inflamed blood vessels is critical for the treatment of the aforementioned diseases as well as for the prevention of rejection of implanted biomaterials [3,7].

Intravital microscopy of live animals has long been used to directly observe the dynamics of leukocytes in inflamed blood vessels, and indeed it has provided phenomenological descriptions of the stunning dynamics of leukocytes so called adhesion cascades including rolling, adhesion, crawling, and transendothelial migration (TEM) [1,2]. However, detailed mechanistic study of each adhesion cascade has not been easy to perform with live animals. As an alternative in vitro system for the mechanistic study of leukocyte dynamics on an inflamed endothelium, parallel plate flow chambers have been widely used [8,9]. In this setting, a confluent layer of endothelial cells (ECs) grown in vitro is assembled with a straight flow channel, and suspension of leukocytes is perfused with a defined flow rate in order to mimic the minimal characteristics of blood vessels [8–10]. While this in vitro model system has been successfully used in elucidating mechanistic details of leukocyte-EC interactions under shear, it does not fully recapitulate all the features of blood vessels in vivo. One of the missing features in the parallel plate flow chambers is the lack of alignment of ECs along the direction of shear flow, since endothelial cells cultured on flat surfaces under static environments grow with random orientation [11,12]. EC alignment in vivo has a close

* Corresponding author. School of Interdisciplinary Bioscience and Bioengineering (I-Bio), Pohang University of Science and Technology (POSTECH), San 31, Hyoja-dong, Nam-Gu, Pohang, Gyeongbuk 790-784, South Korea. Tel.: +82 54 279 2189; fax: +82 54 279 5899.
** Corresponding author. School of Mechanical and Aerospace Engineering, Seoul National University, Seoul 151-742, South Korea. Tel.: +82 288 091 03; fax: +82 288 301 79.
E-mail addresses: sky4u@snu.ac.kr (K.-Y. Suh), jsdoh@postech.ac.kr (J. Doh).
[1] These authors contributed equally to the work.

0142-9612/$ – see front matter © 2011 Elsevier Ltd. All rights reserved.
doi:10.1016/j.biomaterials.2011.12.002

relationship with the streamline of the blood flow determined by Reynolds number and the geometry of the blood vessels; ECs in straight segments of blood vessels are aligned along the direction of blood flow due to the straight streamline of that blood flow, while ECs in more complex-shaped regions of blood vessels, such as vascular bifurcations and curved segments with high curvatures, are poorly aligned due to the complicated streamline of blood flow [13]. Since leukocyte infiltration preferentially occurs at complex-shaped blood vessels where ECs are poorly aligned [14,15], alignment of ECs itself may play an important role in leukocyte infiltration; nevertheless, the role of EC alignment in leukocyte dynamics has not been independently investigated.

ECs can be aligned in vitro by applying mechanical stimulations relevant to the physiological environment of blood vessels, such as shear flow or cyclic strain to a confluent layer of ECs [11,16]. However, these methods typically require more than 10 h of stimulation with specialized devices, and thus may not be suitable for mass production of well-aligned endothelial layers. In contrast, when ECs are grown on surfaces containing nanoscale groove/ridge structures, they spontaneously align with their growth along the direction of the nanogrooves [17,18], allowing for a large number of substrates with well-aligned ECs to be formed in a simple and reproducible manner. Nanostructured surfaces can be readily fabricated in a typical lab setting via various unconventional lithographic methods, such as capillary force lithography (CFL) [18], which has been widely used for the control of various cellular behaviors.

In this study, we sought to understand the role of endothelial cell alignment in leukocyte dynamics by using endothelial layers aligned by nanostructured surfaces. Highly uniform nanoscale ridge/groove structures were fabricated by CFL on glass substrates, and subsequently ECs were aligned by culturing them on the nanostructured surfaces. The dynamics of T cells on ECs aligned by nanostructured surfaces were studied by inserting ECs cultured on nanostructured surfaces into parallel plate flow chambers and performing flow assays. Differences in T cell dynamics on well-aligned and randomly oriented ECs were analyzed, and mechanisms for those differences were further assessed by characterizing the structures of junctions formed among ECs on different types of substrates.

2. Materials and methods

2.1. Nanostructured surface fabrication

Nanostructured surfaces were fabricated by capillary force lithography as described in [17,19]. Silicon masters containing various ridge/groove dimensions, 350 nm/350 nm, 350 nm/700 nm, 350 nm/1050 nm, and 800 nm/800 nm, with height of 500 nm were prepared by standard photolithography and reactive ion etching. Then, 50 μl of polyurethane acrylate (PUA) precursor solution (Minuta Tech, Korea) was drop-dispensed on the silicon master, covered with a transparent poly(ethylene terephthalate) (PET) film of 50 μm thickness, and cured by 30 s of UV exposure ($\lambda = 250-400$ nm, 100 mJ/cm^2, Minuta Tech., Korea). After UV-curing, the PUA mold was peeled off from the silicon master using sharp tweezers and further exposed to UV light for 10 h for complete annihilation of reactive acrylate groups. Thin circular coverslips with diameter 18 mm (Marienfeld) were spin-coated with primer (Minuta Tech., Korea) at 3000 rpm for 20 s and baked at 120 °C for 20 min. Then, 50 μl of PUA precursor solution was drop-dispensed on the primer-coated coverslip and the PUA mold was placed on it. After 30 s of UV exposure, the PUA mold was peeled off, resulting in PUA nanostructured surfaces with identical features and dimensions to the original silicon masters. The PUA-patterned glasses were further exposed to UV for 3 h to completely cure residual chemicals.

2.2. Cell culture

bEnd.3 cells were purchased from ATTC and cultured in DMEM medium (Invitrogen) supplemented with 10% of FBS and 1% of penicillin–streptomycin. To culture bEnd.3 cells on PUA surfaces, substrates were treated with air plasma (200–500 W, Femto Science, Korea) and coated with gelatin by incubating with 0.1% gelatin (Sigma) in DI water for 30 min at 37 °C. Each gelatin-coated substrate was placed in a well of 12-well plates and 1 ml of 2×10^5 cells/ml bEnd.3 cells were added on substrates. Typically, a confluent monolayer of bEnd.3 cells was formed after 2 days of cell culture. DO11.10 T cell receptor transgenic mice were purchased from Jackson Laboratories and bred in the animal care facility in the POSTECH Biotech Center (PBC) under pathogen-free conditions. All experiments involving mice were approved by the Institutional Animal Care and Use Committee at PBC. DO11.10 blasts were prepared by stimulating cells from spleen and lymph node of DO11.10 transgenic mice with 1 μg/ml of OVA323–339 peptide (ISQAVHAAHAEINEAGR, Peptron, Inc. Korea). DO11.10 blasts were grown in RPMI 1640 (Invitrogen) containing 10% of FBS (Gibco), 100 U/ml of penicillin, 100 mg/ml of streptomycin (Invitrogen), and 0.1% of beta-mercaptoethanol (Sigma). On the 2nd day of stimulation, 1–2 U/ml of IL-2 was added and cells on 5–7th days were used for experiments.

2.3. Fluorescence microscope

A modified Zeiss Axio Observer.Z1 epi-fluorescence microscope with 10X (Plan-Neofluar, NA = 0.3), 20X (Plan-Neofluar, NA = 0.5) and 40X (Plan-Neofluar, NA = 1.30) objective lenses and a Roper Scientific CoolSnap HQ CCD camera was used for imaging. An XBO 75 W/2 Xenon lamp (75 W, Osram) and DAPI (EX. 365, BS 395, EMBP445/50), eGFP (EX BP 470/40, BS 495, EMBP 525/50), Cy3 (EX BP 550/25, BS 570, EMBP 605/70), Cy5 (EX BP 620/60, BS 660, EMBP 770/75) filter sets were used for fluorescence imaging. The microscope was automatically controlled by Axiovision 4.6 (Carl Zeiss), and acquired images were analyzed and processed with Methamorph (Universal Imaging, Molecular Devices) or Image J.

2.4. Immunostaining

A monolayer of bEnd.3 cells was fixed with 4% paraformaldehyde for 10 min at room temperature, rinsed with PBS, stained with fluorophore-conjugated antibodies, and examined with fluorescence microscope. For the visualization of adherens junctions, VE-cadherin was stained with anti-VE-cadherin-FITC (clone: eBioBV13, eBioscience). For the quantification of adhesion molecule expression of ECs, bEnd.3 cells were stimulated with TNF-α (10 ng/ml) for 4 h and fixed. Fixed cells were rinsed with PBS and stained with primary and secondary antibodies as follows: for P-selectin and VCAM-1 staining, anti-P-selectin-PE (clone: Psel.KO2.3, eBioscience) and anti-VCAM-1-FITC (clone: 429, eBioscience) were used, respectively. For ICAM-1 staining, anti-ICAM-1 (clone: YN1/1.7.4, eBioscience) and donkey anti-rat-FITC (Jackson ImmunoResearch Laboratories) were used. For E-selectin staining, anti-mouse-E-selectin-biotin (clone: 10E9.6, BD Biosciences) and streptavidin-PE (eBioscience) were used. Fluorescence images of fixed and stained bEnd.3 cells were acquired by optical z-sectioning (5 individual planes, 0.5 μm apart) using a 40X objective lens. Integrated intensities of each molecule along the z-axis were obtained with Image J and Metamorph (Molecular Devices).

2.5. Flow-induced alignment of ECs

To align the confluent layers of ECs by flow, a peristaltic pump (MP-1000, Tokyo Rikakikai), two bottles filled with 10 ml of bEnd.3 culture medium, and a rectangular shear chamber (Chamlide CF, Live Cell Instrument, Korea) with channel dimensions of 0.2 mm (height), 2 mm (width) and 17 mm (length) were serially connected with silicon tubes (inner diameter/outer diameter = 1.15 mm/3.2 mm, Korea Ace) as schematically shown in supplementary Fig. S1. To maintain standard tissue culture conditions (37 °C, 5% CO_2) for ECs in the shear chamber, all the components except the peristaltic pump were kept in a tissue culture incubator, and a small hole was made at the lid of a reservoir bottle for air exchange. For alignment of ECs, a monolayer of bEnd.3 cells was mounted on the shear chamber and 15 dyne/cm^2 of shear stress was applied continuously for 40 h.

2.6. Parallel plate chamber assay

The monolayer of bEnd.3 cells was treated with TNF-α (10 ng/ml) for 4 h, overlaid with a chemokine, either SDF-1 (100 ng/ml, PeproTech) or CCL-21 (5 μg/ml, PeproTech), for 10 min, and mounted on a rectangular shear chamber (Chamlide CF, Live Cell Instrument, Korea) with channel dimensions of 0.2 mm (height), 2 mm (width) and 17 mm (length). DO11.10 T cells harvested from the culture flasks were resuspended into binding medium (cation-free Hank's balanced salt solution contacting 10 mM HEPES at pH 7.4 and 2 mg/ml of bovine serum albumin supplemented with Ca^{2+} and Mg^{2+} at 1 mM each) [9] with concentration of 1.5×10^6 cells/ml after removing dead cells with histopaque (Sigma). DO11.10 T cells in binding medium were perfused over the bEnd.3 cell monolayer using a syringe pump (New Era Pump Systems, US) directly connected to the inlet of the shear chamber. To maintain a constant temperature of 37 °C, inline and stage heaters (Live Cell Instrument, Korea) were used. Initially, DO11.10 blasts in binding medium were injected at 0.25 dyne/cm^2 for 10 min to accumulate DO11.10 blasts on endothelium. Then, shear stress was elevated to 2 dyne/cm^2 for 20 min by perfusing binding medium alone. The dynamics of T cells in the flow chamber were observed using a 20× objective lens by performing time-lapse microscopy with 15 s of interval for 20 min.

3. Results and discussion

3.1. Endothelial cell alignment on nanoscale ridge/groove surfaces

Various sizes of nanoscale ridge/groove surfaces were fabricated by UV-assisted CFL using UV-curable polyurethane acrylate (PUA) [19]. Flat PUA surfaces were also prepared for control experiments. Nanostructured surfaces were formed over the entire coverslips with high fidelity and physical integrity. Representative scanning electron microscope (SEM) images of a nanoscale ridge/groove surface with a 350 nm ridge, 700 nm groove, and 500 nm height are shown in Fig. 1A. Topographical features with four different ridge/groove dimensions, 350 nm/350 nm, 350 nm/700 nm, 350 nm/1050 nm, and 800 nm/800 nm, with constant height (500 nm) were fabricated on the surfaces. bEnd.3 cell, a murine brain endothelial cell line, was used as a model EC. ECs were seeded onto the gelatin-coated nanostructured or flat PUA surfaces, and grown until they formed confluent monolayers. Then, differential interference contrast (DIC) images were acquired with a 10× objective lens and their orientations along the axis of the nanogrooves were examined. ECs cultured on the nanostructured surfaces were aligned well along the direction of the nanogrooves (Fig. 1B), while ECs cultured on the flat surfaces were randomly oriented (Fig. 1C). Endothelial cell alignment was further quantified by measuring the angles between the direction of the nanogrooves and the cell elongation axis, as shown in the cartoon in Fig. 1D. Angles of ~200 cells per each type of surface were measured and angular distributions were plotted in Fig. 1D. As expected, ECs on the flat surfaces exhibited uniform angular distribution, suggesting that they were randomly oriented on the surfaces. In contrast, the majority (>80%) of ECs on the nanostructured surfaces had values between 0° and 10° regardless of the ridge/groove dimensions. Degrees of alignment among different nanostructures used in the experiments were almost identical, and thus only one type of nanoscale ridge/groove structure (350 nm/700 nm) was used for the rest of the experiments. When ECs contact each other, they form adherens junctions mediated by homotypic interactions of VE-cadherin between neighboring ECs, which junctions play a critical role in the integrity of the endothelium [20]. To test whether adherens junction formation is normal for both types of surfaces, we fixed

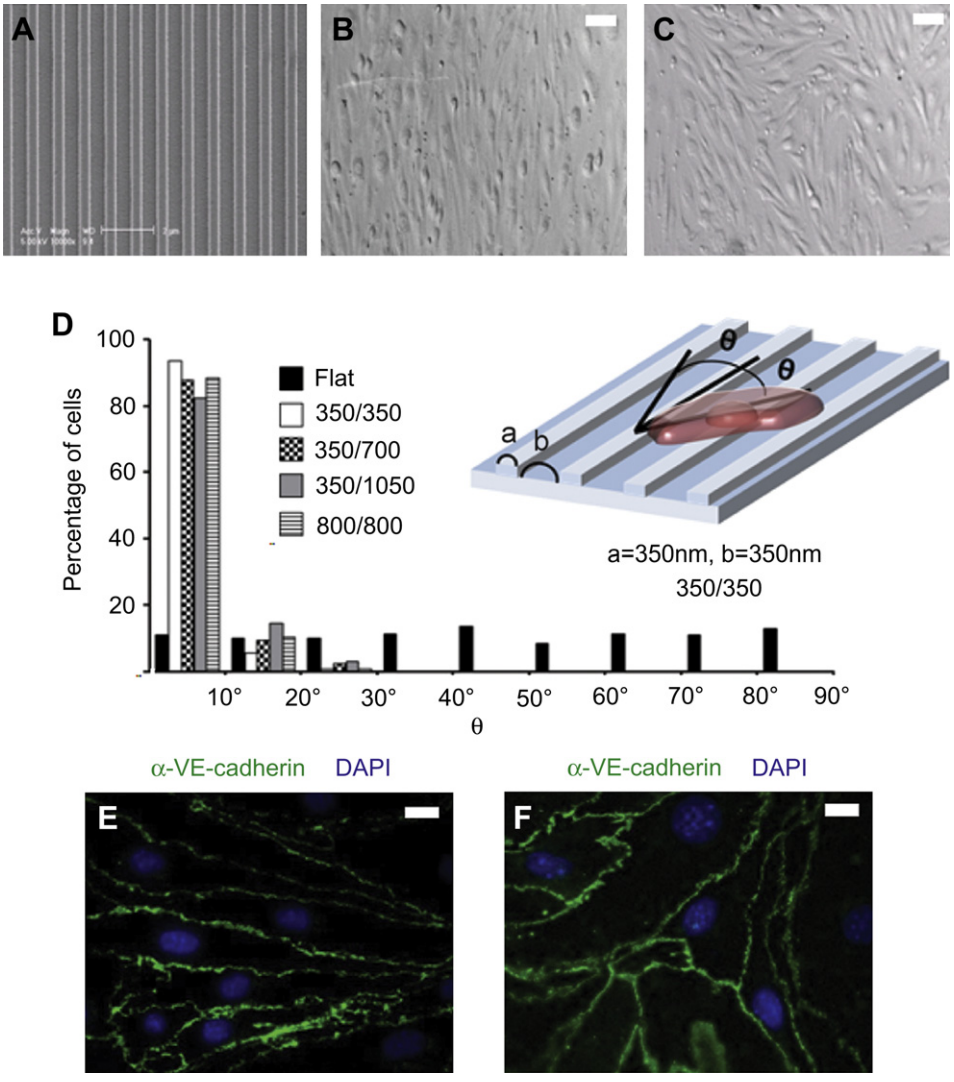

Fig. 1. Alignment of Endothelial cells (ECs) on nanoscale ridge/groove surfaces. (A) SEM image of 350 nm/700 nm ridge/groove surface. (B–C) DIC images of ECs cultured on nanostructured (B) and flat surfaces (C). Scale bar: 50 μm. (D) Angular distribution of ECs cultured on various types of surfaces. (E) Fluorescence image of nucleus (blue) and VE-cadherin (green) stained ECs on nanostructured surfaces. Scale bar: 20 μm. (F) Fluorescence image of nucleus (blue) and VE-cadherin (green) stained ECs on flat surfaces. Scale bar: 20 μm. (For interpretation of the references to colour in this figure legend, the reader is referred to the web version of this article.)

ECs and stained them with fluorophore-conjugated antibody against VE-cadherin. As shown in Fig. 1E–F, clear VE-cadherin staining along the junctions was observed for ECs on both types of surfaces, suggesting that the adherens junction formation was not affected by the surface nanotopography.

3.2. Effect of surface nanotopography on TNF-α responses of ECs

Inflammatory cytokines such as TNF-α and IL-1 trigger upregulation of the many adhesion molecules on ECs involved in leukocyte adhesion cascades such as rolling, adhesion, crawling, and transendothelial migration (TEM) [1–3]. For T cells, P-selectin, E-selectin and vascular cell adhesion molecule 1 (VCAM-1) are important for rolling; VCAM-1 and intercellular adhesion molecule 1 (ICAM-1) are critical for adhesion and crawling; and ICAM-1 is important for TEM [2]. First, we characterized the effect of TNF-α stimulation on adhesion molecule expression of ECs on flat surfaces. ECs cultured on flat PUA surfaces were stimulated with 10 ng/ml of TNF-α for 4 h and expression levels of ICAM-1, VCAM-1, P-selectin, and E-selectin were quantified by immunofluorescence microscopy. Fluorescence images of five z-sections (0.5 μm in distance) near the apical layer of the ECs were acquired from TNF-α-stimulated ECs and unstimulated ECs, and fluorescence intensities over the five z-section images were integrated. Integrated fluorescence intensities were normalized with the values of the unstimulated ECs and plotted in Fig. 2A. As shown, all four molecules were significantly upregulated when ECs were stimulated with TNF-α, as described previously [21].

Next, we compared the expression levels of adhesion molecules of ECs cultured on nanostructured surfaces with those of ECs on flat surfaces. In this case, normalized fluorescence intensity is defined as the relative fluorescence intensity to the fluorescence intensity of flat surfaces, such that all the values for the flat surfaces would be one, and relative differences between nanostructured and flat surfaces could be directly compared. The normalized fluorescence intensity values of all molecules of unstimulated ECs and TNF-α stimulated ECs are plotted in Fig. 2B and C, respectively. Overall, the effect of nanotopography on adhesion molecule expression of ECs was marginal. Without TNF-α treatment, the expression levels of all four molecules of ECs on nanostructured surfaces were identical to those of ECs on flat surfaces (Fig. 2B). When ECs were stimulated with TNF-α, only the expression level of E-selectin of ECs on nanostructured surfaces was slightly higher than that of ECs on flat surfaces (~8%) and expression levels of all the other molecules were comparable. Together, TNF-α treatment significantly increased the adhesion molecule expression of ECs cultured on both flat and nanostructured surfaces while surface nanotopography exhibited minimal effect on the expression level of each adhesion molecule.

3.3. T cell dynamics on inflamed endothelium

As shown in Fig. 3A, T cell adhesion dynamics on an inflamed endothelium are commonly classified into rolling, adhesion, crawling and transendothelial migration (TEM) [1,2,9]. Detachment of T cells can occur in any region of adhesion dynamics when the adhesion force is weaker than the shear force applied by the flow. ECs cultured either on nanostructured or flat surfaces were stimulated with TNF-α for 4 h. As shown above, the expression levels of ICAM-1, VCAM-1, and P-selectin on ECs were not affected by the surface nanotopography, and only E-selectin expression was slightly different depending on the surface nanotopography. Since the major focus of this study is the role of EC alignment on lymphocyte dynamics, the identical expression level of adhesion molecules, which is independent of surface nanotopography, is desirable. Therefore, we decided to focus on later phases of adhesion cascades, crawling and TEM, in which E-selectin expression level on ECs would not play any role. CCL-21 or SDF-1α, chemokines

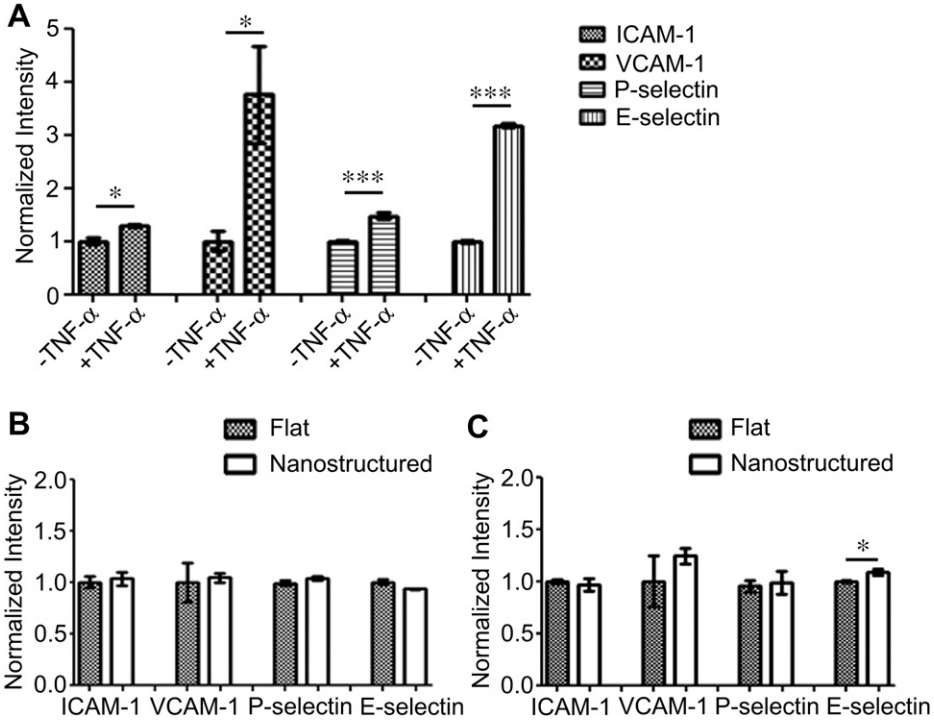

Fig. 2. Effect of surface nanotopography on adhesion molecule expression of ECs. (A) Effect of TNF-α stimulation on adhesion molecule expression of ECs cultured on flat surfaces (B) Effect of nanotopography on adhesion molecule expression of ECs in the absence of TNF-α stimulation. (C) Effect of nanotopography on adhesion molecule expression of ECs in the presence of TNF-α stimulation. ($^{*}p < 0.05$, $^{**}p < 0.01$, $^{***}p < 0.001$).

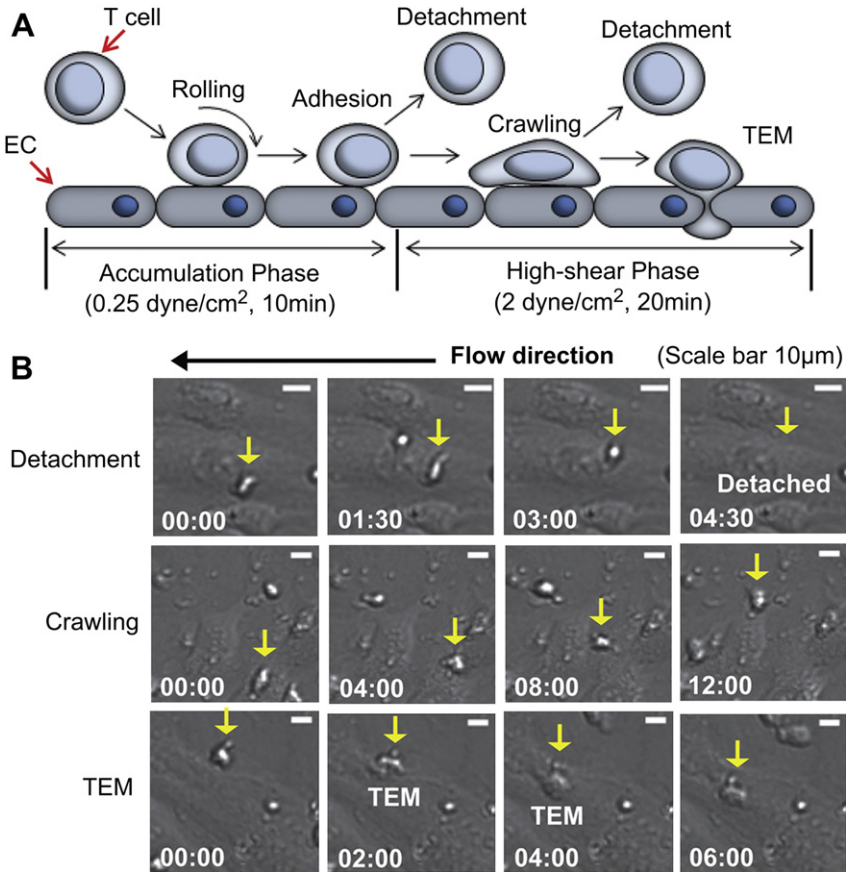

Fig. 3. Dynamics of T cells on ECs. (A) Schematic illustration of experimental procedures and expected dynamics of T cells in each phase of experiment. (B) Time-lapse images of representative states of T cell dynamics. (Experiments were performed on ECs cultured on flat surfaces): detachment (upper row), crawling (middle row) and transendothelial migration (TEM, lower row). Yellow arrows: T cells undergoing each state of dynamics. Elapsed time: mm:ss. (For interpretation of the references to colour in this figure legend, the reader is referred to the web version of this article.)

promoting TEM under shear by activating T cell integrins [9,22] were overlaid on TNF-α stimulated ECs, and a rectangular shear chamber (Chamlide CF, Live Cell Instrument, Korea) with channel dimensions of 0.2 mm (height), 2 mm (width) and 17 mm (length) was assembled on the substrates containing a monolayer of ECs. ECs grown on nanostructured surfaces were inserted into the flow chamber with the direction of the EC alignment either parallel or perpendicular to the direction of the flow. Flow assays were performed as schematically shown in Fig. 3A. First, suspension of DO11.10 T cell blasts (1.5×10^6 cells/ml) in binding media (cation-free Hank's balanced salt solution contacting 10 mM HEPES at pH 7.4 and 2 mg/ml of bovine serum albumin supplemented with Ca^{2+} and Mg^{2+} at 1 mM each) [9] was perfused with low shear stress (0.25 dyn/cm^2) on a monolayer of TNF-α stimulated and chemokine overlaid ECs for 10 min. The majority of T cells under this low shear stress were in either 'rolling' or 'adhesion' states, and only fractions of them underwent further adhesion cascades such as 'crawling' and 'TEM'. As a result, a substantial number of T cells were accumulated on ECs during this 'accumulation phase', as described previously [9]. Subsequently, shear stress was elevated to 2 dyne/cm^2, a typical shear stress value at post-capillary venules used for the assessment of T cell dynamics on ECs [8,9], and dynamics of T cells on ECs were observed by time-lapse microscopy for 20 min. During this 'high-shear phase', weakly adhering T cells were detached, and the majority of T cells began active crawling on ECs in search of sites for TEM. Behaviors of crawling T cells can be divided into three categories: (1) detached from ECs during crawling by flow (upper row of Fig. 3B, the yellow arrowed T cell was disappeared at 4:30, or Video 1 in Supplementary data), (2) continuously crawled on ECs with characteristic hand-mirror shapes over 20 min (middle row of Fig. 3B or Video 2 in Supplementary data), and (3) successfully underwent TEM within given time (lower row of Fig. 3B, the yellow arrowed T cells was slightly under focused at 0:00 and in-focus for the rest of time points, or Video 3 in Supplementary data).

Supplementary data related to this article can be found online at doi:10.1016/j.biomaterials.2011.12.002.

With this experimental scheme, we investigated the role of EC alignment on T cell dynamics. The dynamics of T cells on ECs cultured either on nanostructured or flat surfaces were divided into the three categories described above by analyzing time-lapse images (Fig. 4A). In the case of the T cells on well-aligned ECs by nanostructured surfaces, flow was either applied parallel (nanostructured/parallel) or perpendicular (nanostructured/perpendicular) to the direction of EC alignment; in this case, ~20% of T cells underwent TEM, while ~35% of T cells continuously crawled over 20 min and ~45% of T cells were detached during crawling (slightly higher detachment of T cells was occurred for nanostructured/perpendicular than nanostructured/parallel). In sharp contrast, more than 60% of T cells on randomly oriented ECs cultured on flat surfaces underwent TEM and substantially lower percentage of T cells were either continuously crawling on ECs (~20%) or detached (~15%). Increased detachment of T cells on well-aligned ECs may be mainly due to the fact that they did not undergo TEM as much as

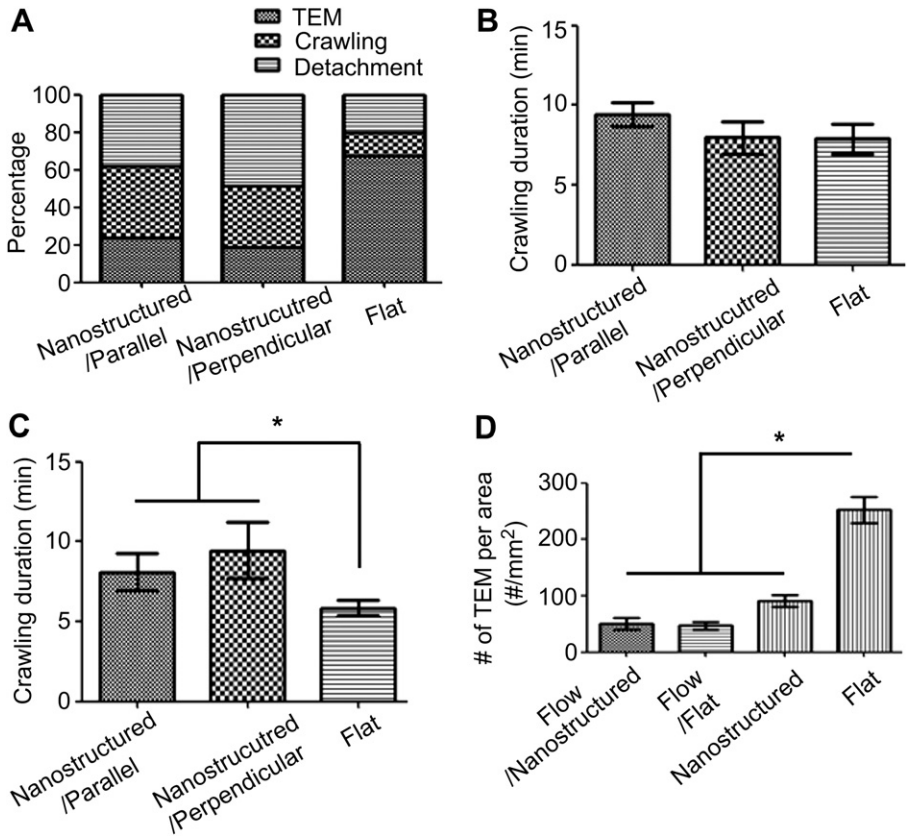

Fig. 4. Effect of EC alignment on T cell dynamics. (A) Percentage of each state of T cell dynamics on ECs cultured on nanostructured and flat surfaces. Parallel and perpendicular, respectively, denote the direction of flow relative to the direction of nanogrooves. (B) Average crawling duration of T cells detached from ECs. (C) Average crawling duration of T cells underwent TEM. (50–60 T cells per each case were evaluated for Fig. 4A–C) (D) Frequency of TEM of T cells per area on EC layers prepared by various methods. ($^{*}p < 0.05$, $^{**}p < 0.01$, $^{***}p < 0.001$).

did the T cells on randomly oriented ECs; thus, the majority of T cells on well-aligned ECs were exposed to shear flow for a longer period of time than were the T cells on randomly oriented ECs. Indeed, when we measured the crawling duration until detachment of T cells on ECs cultured on either nanostructured or flat surfaces, average crawling durations were not significantly different from each other (8–9.5 min, Fig. 4B), supporting this possibility. In contrast, average crawling duration until TEM of T cells was significantly longer for T cells on well-aligned ECs (8.1 ± 1.1 min for nanostructured/parallel and 9.5 ± 1.8 min for nanostructured/perpendicular) than for T cells on randomly oriented ECs (5.8 ± 0.5 min, Fig. 4C). Taken together, T cells on randomly oriented ECs cultured on flat surfaces underwent TEM much more frequently and quickly than T cells on well-aligned ECs cultured on nanostructured surfaces. Finally, to test the physiological relevance of the finding that EC alignment itself can inhibit TEM of T cells, ECs were aligned by flow and the T cell dynamics on flow-aligned ECs were examined. The frequency of TEM of T cells per area on ECs prepared by four different methods, ECs on nanostructured surfaces exposed to the identical amount of shear stress to flow-aligned ECs on flat surfaces (flow/nanostructured), ECs on flat surfaces aligned by flow (flow/flat), ECs aligned by nanostructured surfaces (nanostructured), and ECs randomly oriented on flat surfaces (flat), were measured and data are plotted in Fig. 4D. Regardless of the methods for EC alignment, frequencies of TEM of T cells on well-aligned ECs (flow/nanostructured, flow/flat, and nanostructured) were significantly lower than those of T cells on randomly oriented EC (flat), further supporting the idea that EC alignment is a critical factor regulating TEM of T cells.

3.4. Characteristics of preferential sites for TEM

Leukocytes, including T cells, can across endothelial layers by passing through junctions formed among ECs (paracellular migration), or directly passing through cell bodies of ECs (transcellular migration) [1,2]. In our experimental settings, we mainly observed paracellular migration, and thus we hypothesized that certain characteristic of EC junctions important for TEM of T cells were different between ECs cultured on flat surfaces and ECs cultured on nanostructured surfaces. One of the important factors of EC junctions for leukocyte TEM is the number of ECs surrounding junctions: it was reported that leukocytes preferentially undergo TEM on junctions formed by three adjacent endothelial cells (Tri-EC junctions) compared with junctions formed by two adjacent endothelial cells (Bi-EC junction) [14,23]. As can be seen in Fig. 5A, EC junctions in our experimental settings can be classified into Bi-EC junctions (blue arrows in Fig. 5A) or Multi-EC junctions (junctions formed by more than three adjacent EC cells, yellow arrows in Fig. 5A) depending on the number of ECs surrounding the junctions. To find a correlation between the type of EC junction and the TEM of T cells, immunostaining of VE-cadherin was performed immediately after performing parallel plate chamber assays while flow chambers were mounted on a microscope stage such that fluorescence images of identical field of view to differential interference contrast (DIC) images acquired during flow assays could be acquired. By combining information on DIC and fluorescence images of VE-cadherin, we were able to draw lines depicting EC junctions on the original DIC image and identify the types of junctions, as shown in supplementary Fig. S2. Then, the numbers of

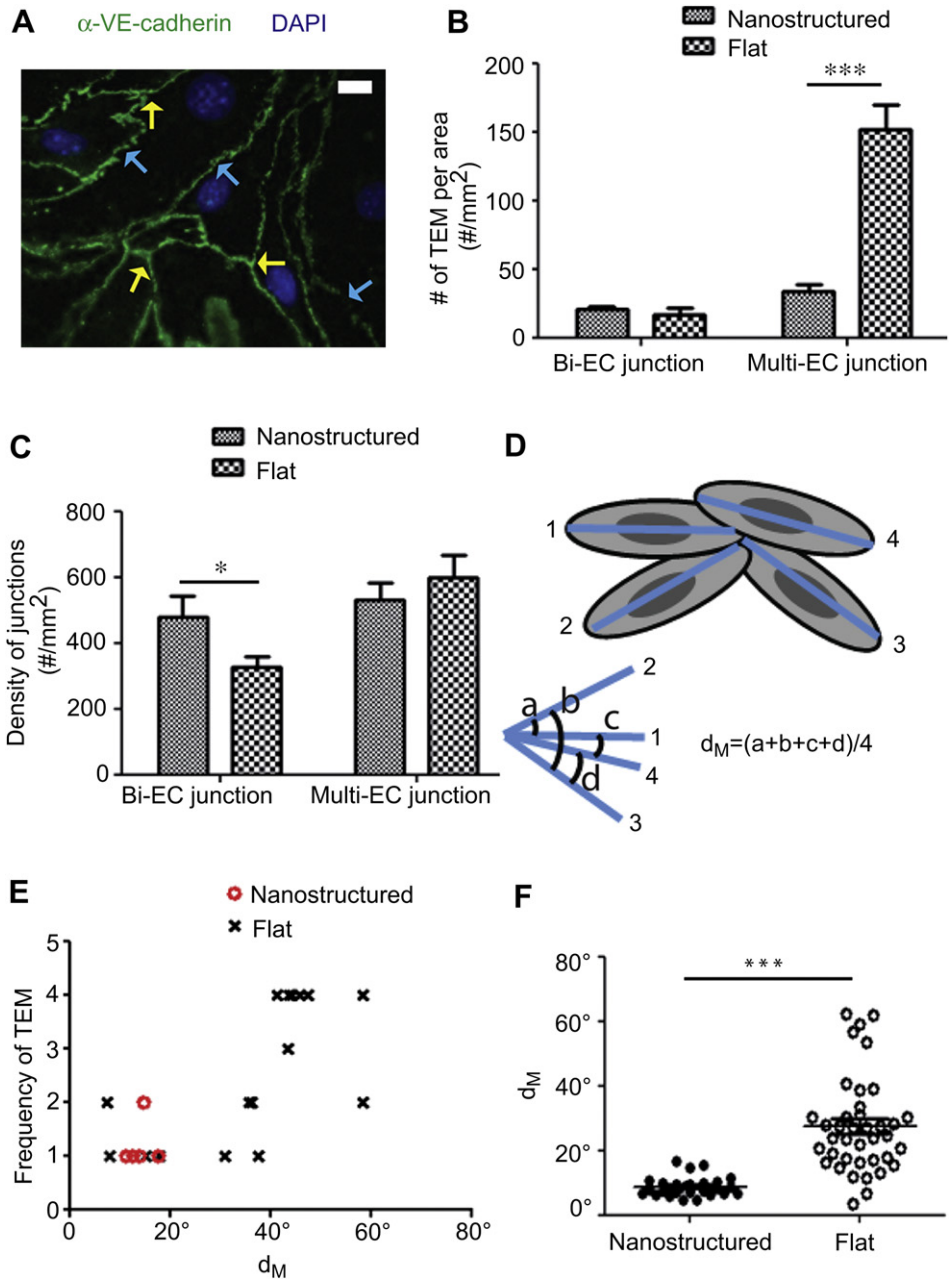

Fig. 5. Characteristics of preferential sites for TEM. (A) Examples of Bi-EC junctions (Blue arrows) and Multi-EC junctions (Yellow arrows) of ECs cultured on flat surfaces. Scale bar: 20 μm. (B) frequency of TEM of T cells per area. (C) Density of Bi-EC junctions and Multi-EC junctions. (D) Schematic illustration of how degree of misalignment (d_M) of ECs surrounding Multi-EC junctions is defined. (E) Correlation between d_M value and frequency of TEM of T cells. (F) Distribution of d_M values of ECs cultured on nanostructured and flat surfaces. ($^{*}p < 0.05$, $^{**}p < 0.01$, $^{***}p < 0.001$). (For interpretation of the references to colour in this figure legend, the reader is referred to the web version of this article.)

TEM per area of each type of junction over 20 min were measured and the data are plotted in Fig. 5B. Notably, the frequency of TEM at Bi-EC junctions was not affected by the type of surfaces used for EC culture, while the frequency of TEM at Multi-EC junctions of ECs cultured on flat surfaces was approximately seven times higher than that of ECs cultured on nanostructured surfaces. Since the density of Multi-EC junctions of ECs on flat surfaces was not significantly different from that of ECs on nanostructured surfaces (Fig. 5), it is likely that Multi-EC junctions of ECs on flat surfaces have certain characteristics for preferential sites of TEM. With careful observation, it was found that TEM of T cells frequently occurred at Multi-EC junctions where the ECs surrounding the junctions were poorly aligned.

Based on our observations, we defined a new parameter d_M for ECs surrounding Multi-EC junctions, as schematically shown in Fig. 5C. This parameter represents the degree of misalignment of junctions relative to each other; we attempted to find a correlation between d_M and TEM for T cells. The orientation of an EC was defined by drawing a line through its long axis, and an acute angle between the lines representing the orientations of two neighboring ECs was measured. The average acute angle of ECs surrounding a Multi-EC junction was designated as d_M; the smaller this d_M value is, the better the local alignment of ECs is, and for the perfectly aligned ECs, $d_M = 0$. Measurement error of this d_M value, estimated by the standard deviation of three independent measurements, was 1.87°. Then, the d_M value of the

Multi-EC junctions where TEM occurred vs. the number of TEM that occurred at those junctions over the experimental time period (20 min) from a representative experimental set was measured and the data are plotted in Fig. 5D to demonstrate a correlation between d_M value and frequency of TEM of T cells. Interestingly, the majority of junctions (higher than 80%) with a d_M value smaller than 40° had only one TEM of T cells per junction. In sharp contrast, the majority of junctions (higher than 80%) with a d_M value higher than 40° had more than three TEM of T cells per junction, implying that Multi-EC junctions surrounded by poorly aligned ECs form 'preferential sites for TEM'. When we examined d_M values of Multi-EC junctions, approximately 15% of Multi-EC junctions on flat surfaces had d_M values higher than 40°, while all Multi-EC junctions on nanostructured surfaces had d_M values smaller than 40° (Fig. 5F). This suggests that a higher frequency of TEM of T cells occurred on ECs cultured on flat surfaces because ECs on such surfaces contained many more 'preferential sites for TEM'. The exact mechanism that determines why TEM of T cells preferentially occurred at Multi-EC junctions with d_M values higher than 40° remains to be determined. One possibility is that the distribution of key molecules for TEM of T cells at the Multi-EC junctions might depend on the alignment of ECs surrounding the junctions. While the molecular mechanism of TEM of T cells has not been completely understood [24], we used immunofluorescence microscopy to examine the distribution of ICAM-1 and CD99, which were suggested to be important for TEM of T cells [14,25], but did not notice any distinct distribution of these molecules near the Multi-EC junctions with d_M values higher than 40° (data not shown). Alternatively, poorly aligned Multi-EC junctions might provide better structural support for force transduction of T cells to squeeze them into the junctions, and thus to facilitate the TEM of T cells.

Disruption of EC alignment and increase of d_M values may occur during inflammation. Various inflammatory mediators trigger vascular widening so called vasodilation, which significantly increases the diameter of vessels [26]. As a result, the acute angle increases between adjacent ECs and the d_M values are also likely to increase. Increased d_M values would significantly increase the number of 'preferential sites for TEM' for leukocytes, and would thus enhance TEM and tissue infiltration of leukocytes. This may provide new insights into the mechanism of extravasation of leukocytes in inflamed vessels.

The result that aligned ECs allowed less TEM than did randomly oriented ECs may suggest a new strategy for the design of small diameter synthetic vascular grafts. Massive clot formation is one of the major causes of small diameter synthetic vascular graft failure. To minimize thrombosis in such synthetic vessels, the luminal surfaces of synthetic vessels have often been coated with a monolayer of ECs [6]. However, detachment of ECs by endothelia-infiltrated leukocytes, particularly at early stages of implantation, is one of the serious issues to be resolved for the success of this strategy [27,28]. Here, we demonstrated that aligned ECs cultured on nanostructured surfaces could substantially reduce TEM of T cells, suggesting leukocyte infiltration of synthetic grafts coated with ECs could be minimized by introducing nanotopography to the inner wall of synthetic vessels so that ECs could be elongated and aligned to the direction of flow from the beginning of implantation. In addition, our previous research demonstrated that EC detachment by shear flow could be minimized by modulating the dimensions of nanoscale ridges and grooves [17], and thus that the introduction of well-aligned nanostructures to the inner surfaces of small diameter vascular grafts for the attachment of ECs would be an attractive strategy that could minimize leukocyte infiltration as well as improve EC adhesion.

4. Conclusions

In summary, we have investigated the role of endothelial cell alignment on T cell dynamics by integrating nanostructured surfaces inside a fluidic chamber. By comparing T cell dynamics on well-aligned ECs cultured on nanostructured surfaces with those on randomly oriented ECs cultured on flat surfaces, we demonstrated that EC alignment is important for the regulation of TEM of T cells; T cells preferentially underwent TEM at junctions surrounded by more than three ECs only if ECs surrounding those junctions were poorly aligned along the junctions. This result will suggest a new strategy for the design of synthetic small diameter vascular grafts and extend our current knowledge of leukocyte dynamics on an inflamed endothelium.

Acknowledgments

This work was supported by the Basic Science Research Program (Grant No. 2009-0065183 and 2010-0027955), the Converging Research Center Program (2011K000815) and the World Class University Program (R31-2008-000-10105-0 and R31-2008-000-10083-0) through the National Research Foundation of Korea (NRF), funded by the Ministry of Education, Science and Technology.

Appendix. Supplementary material

Supplementary data related to this article can be found online at doi:10.1016/j.biomaterials.2011.12.002.

References

[1] Nourshargh S, Hordijk PL, Sixt M. Breaching multiple barriers: leukocyte motility through venular walls and the interstitium. Nat Rev Mol Cell Biol 2010;11(5):366–78.
[2] Ley K, Laudanna C, Cybulsky MI, Nourshargh S. Getting to the site of inflammation: the leukocyte adhesion cascade updated. Nat Rev Immunol 2007;7(9):678–89.
[3] Luster AD, Alon R, Von Andrian UH. Immune cell migration in inflammation: present and future therapeutic targets. Nat Immunol 2005;6(12):1182–90.
[4] Luster AD. Chemokines – chemotactic cytokines that mediate inflammation. New Engl J Med 1998;338(7):436–45.
[5] Tabas I. Macrophage death and defective inflammation resolution in atherosclerosis. Nat Rev Immunol 2009;10(1):36–46.
[6] Khan OF, Sefton MV. Endothelialized biomaterials for tissue engineering applications in vivo. Trends Biotechnol 2011;29(8).
[7] Yonekawa K, Harlan JM. Targeting leukocyte integrins in human diseases. J Leukoc Biol 2005;77(2):129.
[8] Steiner O, Coisne C, Cecchelli R, Boscacci R, Deutsch U, Engelhardt B, et al. Differential roles for endothelial ICAM-1, ICAM-2, and VCAM-1 in shear-resistant T Cell arrest, polarization, and directed crawling on blood-brain barrier endothelium. J Immunol 2010;185(8):4846.
[9] Cinamon G, Shinder V, Alon R. Shear forces promote lymphocyte migration across vascular endothelium bearing apical chemokines. Nat Immunol 2001;2(6):515–22.
[10] Luu NT, Rainger GE, Buckley CD, Nash GB. CD31 regulates direction and rate of neutrophil migration over and under endothelial cells. J Vasc Res 2000;40(5):467–79.
[11] Malek AM, Izumo S. Mechanism of endothelial cell shape change and cytoskeletal remodeling in response to fluid shear stress. J Cell Sci 1996;109:713–26.
[12] Azuma N, Akasaka N, Kito H, Ikeda M, Gahtan V, Sasajima T, et al. Role of p38 MAP kinase in endothelial cell alignment induced by fluid shear stress. Am J Physiol-Heart C 2001;280(1):H189.
[13] Langille BL, Adamson S. Relationship between blood flow direction and endothelial cell orientation at arterial branch sites in rabbits and mice. Circ Res 1981;48(4):481–8.
[14] Sumagin R, Sarelius IH. Intercellular adhesion molecule-1 enrichment near tricellular endothelial junctions is preferentially associated with leukocyte transmigration and signals for reorganization of these junctions to accommodate leukocyte passage. J Immunol 2010;184(9):5242.
[15] Tousi N, Wang B, Pant K, Kiani MF, Prabhakarpandian B. Preferential adhesion of leukocytes near bifurcations is endothelium independent. Microvasc Res 2010;80(3):384–8.

[16] Matsumoto T, Yung YC, Fischbach C, Kong HJ, Nakaoka R, Mooney DJ. Mechanical strain regulates endothelial cell patterning in vitro. Tissue Eng 2007;13(1):207–17.
[17] Hwang SY, Kwon KW, Jang KJ, Park MC, Lee JS, Suh KY. Adhesion assays of endothelial cells on nanopatterned surfaces within a microfluidic channel. Anal Chem 2010;82(7):3016–22.
[18] Liliensiek SJ, Wood JA, Yong J, Auerbach R, Nealey PF, Murphy CJ. Modulation of human vascular endothelial cell behaviors by nanotopographic cues. Biomaterials 2010;31(20):5418–26.
[19] Suh KY, Park MC, Kim P. Capillary force lithography: a versatile tool for structured biomaterials interface towards cell and tissue engineering. Adv Funct Mater 2009;19(17):2699–712.
[20] Corada M, Mariotti M, Thurston G, Smith K, Kunkel R, Brockhaus M, et al. Vascular endothelial-cadherin is an important determinant of microvascular integrity in vivo. P Natl Acad Sci USA 1999;96(17):9815.
[21] Sikorski E, Hallmann R, Berg E, Butcher E. The Peyer's patch high endothelial receptor for lymphocytes, the mucosal vascular addressin, is induced on a murine endothelial cell line by tumor necrosis factor-alpha and IL-1. J Immunol 1993;151(10):5239.
[22] Peled A, Grabovsky V, Habler L, Sandbank J, Arenzana-Seisdedos F, Petit I, et al. The chemokine SDF-1 stimulates integrin-mediated arrest of CD34+ cells on vascular endothelium under shear flow. J Clin Invest 1999;104(9):1199.
[23] Burns AR, Walker DC, Brown ES, Thurmon LT, Bowden RA, Keese CR, et al. Neutrophil transendothelial migration is independent of tight junctions and occurs preferentially at tricellular corners. J Immunol 1997;159(6):2893.
[24] Muller WA. Mechanisms of leukocyte transendothelial migration. Annu Rev Pathol-Mech 2011;6(1).
[25] Mamdouh Z, Mikhailov A, Muller WA. Transcellular migration of leukocytes is mediated by the endothelial lateral border recycling compartment. J Exp Med 2009;206(12):2795.
[26] Bagher P, Segal SS. Regulation of blood flow in the microcirculation: role of conducted vasodilation. Acta Physiol 2011;202:271–84.
[27] Herring MB, Compton R, Legrand DR, Gardner AL. Endothelial cell seeding in the management of vascular thrombosis. Semin Tromb Haemost 1989;15: 200–5.
[28] Emerick S, Herring M, Arnold M, Baughman S, Reilly K, Glover J. Leukocyte depletion enhances cultured endothelial retention on vascular prostheses. J Vasc Surg 1987;5(2):342.